Weak Simulated Extratropical Responses to Complete Tropical Deforestation

KIRSTEN L. FINDELL AND THOMAS R. KNUTSON

NOAA/Geophysical Fluid Dynamics Laboratory, Princeton University, Princeton, New Jersey

P. C. D. MILLY

U.S. Geological Survey, NOAA/Geophysical Fluid Dynamics Laboratory, Princeton University, Princeton, New Jersey

(Manuscript received 6 May 2005, in final form 22 September 2005)

ABSTRACT

The Geophysical Fluid Dynamics Laboratory atmosphere–land model version 2 (AM2/LM2) coupled to a 50-m-thick slab ocean model has been used to investigate remote responses to tropical deforestation. Magnitudes and significance of differences between a control run and a deforested run are assessed through comparisons of 50-yr time series, accounting for autocorrelation and field significance. Complete conversion of the broadleaf evergreen forests of South America, central Africa, and the islands of Oceania to grasslands leads to highly significant local responses. In addition, a broad but mild warming is seen throughout the tropical troposphere (<0.2°C between 700 and 150 mb), significant in northern spring and summer. However, the simulation results show very little statistically significant response beyond the Tropics. There are no significant differences in any hydroclimatic variables (e.g., precipitation, soil moisture, evaporation) in either the northern or the southern extratropics. Small but statistically significant local differences in some geopotential height and wind fields are present in the southeastern Pacific Ocean. Use of the same statistical tests on two 50-yr segments of the control run show that the small but significant extratropical differences between the deforested run and the control run are similar in magnitude and area to the differences between nonoverlapping segments of the control run. These simulations suggest that extratropical responses to complete tropical deforestation are unlikely to be distinguishable from natural climate variability.

1. Introduction

Many previous modeling studies have shown that tropical deforestation leads to dramatic changes in local and regional energy and water budgets (e.g., early studies by Henderson-Sellers and Gornitz 1984; Dickinson and Henderson-Sellers 1988; and others mentioned below), but the question of extratropical responses to tropical deforestation has received only limited attention. When forests are converted to croplands and pastures, a number of physical and physiological characteristics change; in our model, these are represented through a decrease in the root-zone water capacity, an increase in the albedo, a decrease in the roughness length, and an increase in the stomatal resistance. Though most studies have shown that these changes lead to increases in local temperatures, the local precipitation response differs from study to study and from region to region. Many studies documented a decrease in atmospheric moisture convergence (Lean and Warrilow 1989; Shukla et al. 1990; Henderson-Sellers et al. 1993), but a few showed an increase (Polcher and Laval 1994) or some areas of increase and other areas of decrease (McGuffie et al. 1995). Shukla et al. (1990) and Henderson-Sellers et al. (1993) saw changes in the Walker and Hadley circulations and hypothesized that these circulatory changes could lead to significant extratropical responses, but neither group was able to test this hypothesis with the simulations available at the time. McGuffie et al. (1995), Sud et al. (1996), and Zhang et al. (1996b) addressed this hypothesis and documented some extratropical responses to tropical deforestation. Other, more recent studies (Chase et al. 2000) focused on actual observed land-use change on a global scale, but linked some of the extratropical responses to tropically forced mechanisms. Computing resources, however, were highly limited in all of the

Corresponding author address: Dr. Kirsten L. Findell, NOAA/Geophysical Fluid Dynamics Laboratory, Princeton University, P.O. Box 308, Princeton, NJ 08542.
E-mail: kirsten.findell@noaa.gov

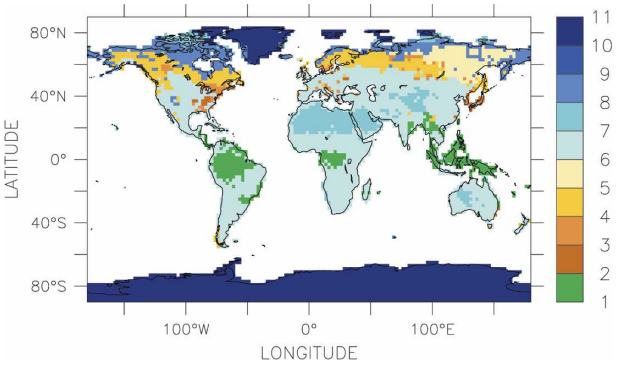

FIG. 1. Cover-type fields in the control run. Vegetation types used in the model are (1) broadleaf evergreen trees, (2) broadleaf deciduous trees, (3) broadleaf–needleleaf trees, (4) needleleaf evergreen trees, (5) needleleaf deciduous trees, (6) grassland, (7) desert, (8) tundra, and (10) ice (type 9 is not used). In the deforested run all broadleaf evergreen trees (type 1) are converted to grasslands (type 6).

above-mentioned studies: they were all integrated for relatively short periods of time (many for less than 5 yr), and most were run at coarse vertical and horizontal resolutions.

Given the limited integration periods of previous studies of tropical deforestation, it seems important to readdress the question of extratropical responses to tropical deforestation. The work presented here attempts to provide a rigorous assessment of the statistical significance of an extratropical response to large-scale tropical deforestation as simulated in the Geophysical Fluid Dynamics Laboratory (GFDL) atmosphere–land model version 2 (AM2/LM2) coupled to a slab ocean model. For the purposes of this paper, the northern and southern extratropics are defined as north of 30°N and south of 30°S, respectively. The deforestation experiment consisted of a complete conversion of all tropical broadleaf evergreen forests to grasslands (Fig. 1). The model is run with a grid spacing of 2° latitude × 2.5° longitude and 24 atmospheric levels. The comparison periods are 50 yr in both the control and the deforestation runs, after spinup periods of 50 and 20 yr, respectively. For comparison, the McGuffie et al. (1995) study compared a 14-yr control run with a 6-yr deforestation run. Their simulations were performed with a modified version of the National Center for Atmospheric Research (NCAR) Community Climate Model (CCM1-Oz) run at R15 truncation (4.5° latitude × 7.5° longitude). The Zhang et al. (1996b) study used these same simulations but continued them for 25 and 11 yr. The Sud et al. (1996) study used 3-yr control and deforested runs with a version of the Goddard Laboratory for Atmospheres (GLA) GCM, run at 4° latitude × 5° longitude resolution with 17 vertical levels. Finally, the Chase et al. (2000) study compared 10 Januaries of results from the NCAR CCM3 model with prescribed annually repeating sea surface temperatures (SSTs). The longer integrations used in this work provide an improved statistical foundation for determining the significance of the results.

The next three sections include brief descriptions of the model, the experimental design, and the statistical techniques used in this study. Section 5 includes a presentation of the results, with a focus on the extratropics. Discussion and conclusions are presented in sections 6 and 7.

2. Model description

The model used, AM2, is a newly developed atmospheric general circulation model coupled to a slab ocean model. The details of the atmospheric model are presented in a paper from the GFDL Global Atmospheric Model Development Team (2004, hereafter GAMDT04). The model is identical to the CM2.0 coupled model of Delworth et al. (2006), except for the use of the slab ocean model and with time-varying forcing fields fixed at 1990 settings (e.g., land use, CO_2). The atmospheric resolution is 2° latitude × 2.5° longitude, with 24 vertical levels. The model has both a seasonal and a diurnal cycle of insolation. The model includes a large-scale cloud scheme with separate prognostic variables for cloud liquid, cloud ice, and cloud fraction. The simulations do not account for the release of carbon that would accompany such large-scale deforestation.

The land model LM2 is based on the Land Dynamics (LaD) model (Milly and Shmakin 2002a), with modifications prompted by coupling to and tuning with AM2 (see GAMDT04). LM2 includes three lumped water reservoirs: snowpack, soil water (root-zone water), and groundwater. For this study, LM2 is run with the same horizontal grid as AM2. Energy is stored as sensible heat in 18 soil layers and as latent heat of fusion in snowpack and all soil layers except the top layer. A non-water-stressed stomatal resistance and a soil–water-stress function limit evapotranspiration. Drainage of soil water to groundwater occurs when the water capacity of the root zone is exceeded, and groundwater discharge to surface water is proportional to groundwater storage. Surface water is routed instantaneously to ocean destination points on the basis of specified drainage basins. Model parameters, including the root-zone water capacity, are dependent on vegetation and soil types; they are spatially varying but temporally constant, with 1990-based cover types determined from the dataset of Hurtt et al. (2006). Cover types for the de-

forested run are derived from this 1990 state, as described below.

In GAMDT04, the AM2/LM2 model configuration is shown to respond realistically to tropical SST anomalies in a 10-member ensemble of fixed SST experiments using SST observations from 1951 to 2000. Extensive discussion in GAMDT04 of tropical and extratropical responses to Pacific SST variations associated with the El Niño phenomenon showed that the atmospheric component of the model is capable of realistically simulating teleconnections between the Tropics and the extratropics.

In our study, the atmospheric model is coupled to a 50-m-thick slab "mixed layer" model of the ocean. Atmosphere and ocean interact through exchanges of sensible, latent, and radiative heat. In addition, the temperature of the slab ocean is influenced by a heat flux adjustment that accounts for the lack of ocean dynamics and other deficiencies in the model. The same heat flux adjustments are used in the control and deforestation runs under the assumption that the horizontal heat transport by ocean currents does not change in these experiments. This methodology is a well-established means of running equilibrium climate experiments (see, e.g., Broccoli 2000; Wilson and Mitchell 1987; Hansen et al. 1984). Further details of the slab model experimental methodology will be reported in a separate publication. The ocean model is coupled to the Sea Ice Simulator (SIS; Winton 2000), a dynamic–thermodynamic sea ice model that calculates the concentration, thickness, temperature, brine content, and snow cover of five ice thickness categories (including open water) as well as the motion of the complete pack.

3. Experimental design

The control simulation (CTL) in this suite of experiments was run for over 100 yr and approximate SST equilibrium was reached after about 20 yr. A full tropical deforestation run (Deforest) with the broadleaf evergreen of the South America, central Africa, and Oceania all replaced with grasslands (Fig. 1) was initialized from the end of the control run and was run for 70 yr. Comparisons were performed on the final 50 yr of each run. Parameters for each cover-type class were originally specified in Milly and Shmakin (2002a), refined slightly in Milly and Shmakin (2002b), and retuned upon coupling with the atmospheric model, as documented in GAMDT04. Replacement of tropical broadleaf evergreen trees with grasslands increases the surface albedo from 0.149 to 0.182, decreases the surface roughness length from 2.65 to 0.07 m, increases the minimum bulk stomatal resistance from 8.7 to 11.3 s m^{-1}, and decreases the effective rooting depth from about 1.3 to 1.0 m. This rooting-depth change has a proportionate effect on the root-zone water capacity of the ground surface, which is also dependent on the soil type.

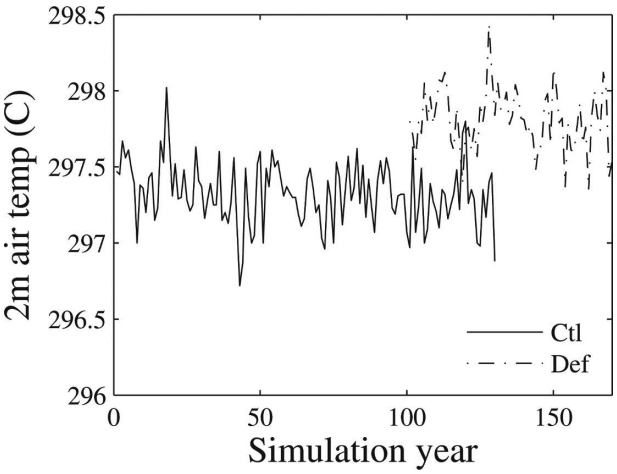

FIG. 2. Average annual 2-m air temperature (°C) in the Amazon basin (20°S–10°N, 80°–40°W) in the full control run (Ctl, 130 yr) and the deforested run (Def, 70 yr, initialized from 1 January, 101 of the control run).

These cover-type changes are expected to produce large changes in each of the deforested regions, as demonstrated in the plot of 2-m air temperature in northern South America for both runs (Fig. 2). A detailed account of the behavior of each region will be provided in a separate publication: the focus of this manuscript is on the extratropical response. We will present some general results for the globe and the Tropics, while highlighting the response in the northern and southern extratropics.

4. Statistical techniques

Because a key aspect of this study is an assessment of whether a statistically significant response is simulated in the extratropics, here we present some detailed discussion of the statistical techniques employed for the study.

a. Accounting for temporal autocorrelation

Following the methodology of Zwiers and Von Storch (1995) and Von Storch and Zwiers (1999), we determine statistical significance of differences between the mean states of our experiments with a modified Student's t test. A critical assumption of a standard t test is independence of samples from different points in a time series. For an autocorrelated time series, this assumption is not valid, and the effective number of

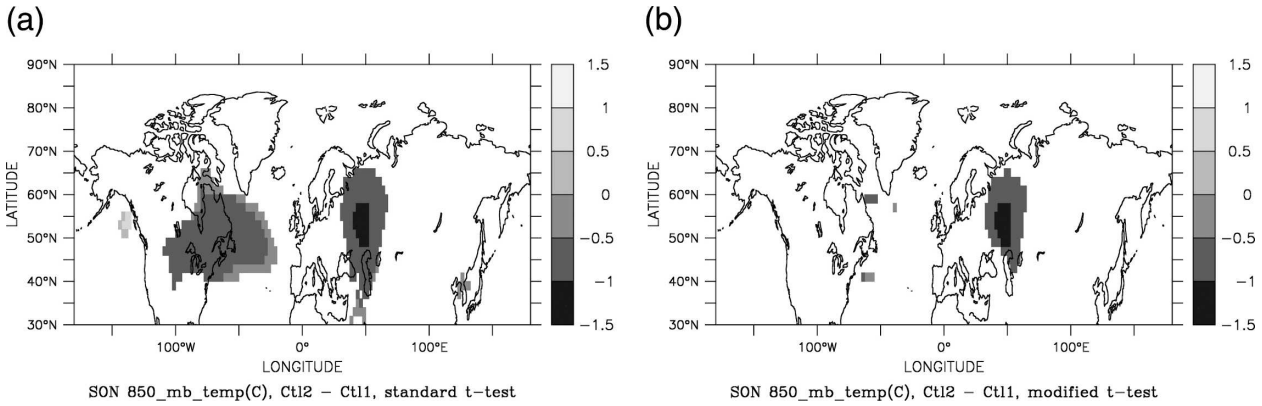

FIG. 3. Comparison of northern extratropical 850-mb temperature difference fields of SON climatologies of two different 50-yr segments of a control run when (a) the standard *t* test is used, and (b) the modified *t* test is used. Differences are only shown where they pass the respective significance tests at the 95% level. In (a) 14% of the surface area passes the standard test; in (b) 3% passes the modified test.

degrees of freedom (dof) is smaller than the total number of points in time in the overall sample. In general, the variance of an autocorrelated series is smaller than that of an uncorrelated series. This means that the standard *t* statistic would be overestimated, and the null hypothesis—that the mean values of the time series are equal—would be rejected more frequently than it should be. In the context of this work, a standard *t* test would be biased toward concluding that a significant climate change had been detected.

Zwiers and Von Storch (1995) and Von Storch and Zwiers (1999) present a method to account for autocorrelation within the time series being compared. They compare a standard *t* statistic to an alternative critical *t* value that was determined from a Monte Carlo experiment where they generated random time series for autoregressive processes of first order with a specified lag-1 autocorrelation. This methodology reduces the number of false rejections of the null hypothesis by accounting for time dependence within the series.

b. Accounting for spatial correlation

Neither the standard nor the modified *t* tests accounts for spatial correlation within fields (Von Storch and Zwiers 1999). Variables such as 500-mb geopotential height have large correlation length scales, meaning that data from adjacent model grid points are not independent, and the effective number of spatial dof is much smaller than the number of grid points. Because of this interdependence between grid points, more than 5% of the area of interest must pass the 95% significance test for the field result as a whole to be statistically significant. Livezey and Chen (1983) present a methodology for determining field significance through an application of the binomial theorem. In their Fig. 3, they show the relation between the number of spatial dof and the estimated percent of local (e.g., at a model grid point) 95% significance tests passed that will be equaled or exceeded by chance 5% of the time. This plot shows that for a field with 40 dof, 12.5% of the field must pass local 95% significance tests for the result as a whole to be statistically significant at the 95% level. Similarly, a field with 20 dof requires about 15% of the field to pass the individual 95% significance tests; 100 dof requires about 9.5% to pass; 200 dof requires about 8% to pass; and 1000 dof requires about 6% to pass.

To apply the Livezey and Chen (1983) results to this study, estimates of the effective dof are needed for each variable and season considered in the two separate extratropical domains. A full Monte Carlo simulation would be required to obtain these values directly; instead, we used published estimates for approximate dof suitable for this study. These published estimates are summarized in the appendix. The reported dof values range from about 20 to about 100, depending on variable, season, and spatial and temporal scales. Though these studies do not provide independent dof estimates for the northern and southern extratropics for all variables, they do give approximate bounds on the dof for many fields. We will use these bounds to guide interpretation of the results presented in the next section.

c. Control–control benchmark comparison

To test the performance of the modified test and the field significance guidelines presented above, two separate 50-yr segments of the control run were compared to provide benchmark values to indicate how much of the area of the earth passes both the standard and

modified *t* tests for a given significance level. A thorough assessment of significance in the deforested–control comparison would require Monte Carlo–type experiments using a long control run so that one could develop a statistical distribution of expected passing rates for each variable and each season independently. Such an analysis would also address the different scales of spatial correlation from variable to variable. Given the relatively small magnitudes of changes and the limited spatial coverage of locally significant differences between the deforested and control runs (shown in the next section), we have not performed such comprehensive tests for this study. Instead, we present seasonal data tables with percent area passing both tests, and mean absolute differences for both the control–control comparison and the control–deforestation comparison (Tables 1 and 2 for the northern and southern extratropics, respectively). Without the full Monte Carlo experiment, we cannot rule out the possibility of statistical significance, but the data tables should allow us to determine whether the extratropical response to tropical deforestation is of practical significance; that is, if such a signal is likely to be distinguishable from natural climate variability on the scale of 50 yr. Again, we stress that we present data from just one control–control comparison: this does not reflect the full range of differences possible in a longer control run.

There is minimal long-term drift in the control run (see, e.g., the plot of the 2-m air temperature in northern South America in Fig. 2), so that any values that pass the significance tests are assumed to arise by chance due to internal variability. The area of the Northern Hemisphere extratropical 850-mb temperature signal for September–November (SON) that passes the standard and modified tests at the 95% significance level in shown in Fig. 3. Fourteen percent of the globe passes the standard test (Fig. 3a), but only 3% passes the modified test (Fig. 3b). Table 1 lists the percent of northern extratropical area that passes these tests for 21 different variables for each of the four seasons for both the control–control comparison and the control–deforested comparison. For the SON season, 16 of the 21 variables have more than 5% of the area passing the standard test in the control–control comparison, but only three variables have more than 5% of the area passing the modified test.

The control–control comparison columns in Tables 1 and 2 (northern and southern extratropics, respectively) make it clear that the percent area passing either significance test is in itself a random variable that has a probability density function (PDF) with values that can be quite different from the expected value of 5%. The standard *t* test frequently has more than 5% of the area passing, as expected due to the lack of independence between points within the time series. The modified test, however, commonly has less than 5% passing, and only rarely has more than 5%, suggesting that the modified test may be overly strict. Given these differences, results of both tests are presented for both hemispheres and for all seasons. Mean absolute differences are also tabulated for each variable; for the hydroclimatic variables (first five lines), they are given as a percentage of the control mean absolute value for ease of interpretation. It is worth noting that for the control–control comparison and the standard *t* test, the eight values (one for each season and hemisphere) show differences across the variables. For example, SST always has more than 5% area passing, and 2 of the 8 values are greater than 20%. The 10-m meridional velocity (10-m vcomp), on the other hand, ranges from 2% to only 8% passing. The geopotential height fields tend to exhibit the largest variations from season to season (e.g., 200-mb geopotential height ranges from 0% to 27% passing). The greatest variation in passing rates, however, is a function of season and hemisphere, with the most extreme examples in northern extratropical June–August (JJA), where all variables in the control–control comparison have more than 5% of area passing the standard *t* test, and in southern extratropical SON, where only SST has more than 5% passing.

5. Deforestation experiment results

One of the most substantial changes that results from a conversion of forests to grassland in the model is the reduction of water available to the vegetation through the roots. This typically leads to a reduction in evapotranspiration (ET) and an increase in sensible heat flux. Since radiation can also change as a result of albedo and cloud changes, it is useful to look at changes in ET relative to changes in net radiation. Conversion of tropical broadleaf evergreen forests to grassland reduces the proportion of the annual mean net radiation at the surface going into ET in each of the deforested regions in the model (Fig. 4). Indeed, this change is extensive in all seasons. However, regional orography, the proximity of oceanic sources of moisture, and the extent of deforestation are quite different in Amazonia, central Africa, and Oceania; as a result, local responses in the three regions are substantially different. In general, the drying is accompanied by a significant warming at the surface, a decrease in evaporation, and an increase in sensible heat flux. The warming can be seen in the time series of annual mean 2-m air temperature in northern South America (Fig. 2) and in the map of annual mean differences showing greater than 1°C

TABLE 1. Mean absolute differences and percentage area of the northern extratropics (north of 30°N) passing the 95% significance tests for four seasons (DJF, MAM, JJA, and SON). Each comparison period is 50 yr long (49 yr used in DJF calculations). From the 130-yr control run, Ctl1 is years 31–80, Ctl2 is years 81–130, and Ctl is years 51–100. Def is the last 50 yr of a 70-yr run. Values exceeding 9.5% (would be significant if there were ~100 spatial dof) are in italics; exceeding 12.5% (~40 dof): bold italics; exceeding 15% (~20 dof): underlined bold italics. For the top five lines, mean absolute differences are presented as percent of control (divided by control mean absolute values and multiplied by 100). Height: geopotential height; SST: sea surface temperature; ucomp: zonal component of the wind; vcomp: meridional component of the wind.

	DJF						MAM					
	Mean absolute differences (% of Ctl for top 5 lines, physical units for others)		Passes standard test (% area)		Passes modified test (% area)		Mean absolute differences (% of Ctl for top 5 lines, physical units for others)		Passes standard test (% area)		Passes modified test (% area)	
Variable	Ctl2 − Ctl1	Def − Ctl	Ctl2 − Ctl1	Def − Ctl	Ctl2 − Ctl1	Def − Ctl	Ctl2 − Ctl1	Def − Ctl	Ctl2 − Ctl1	Def − Ctl	Ctl2 − Ctl1	Def − Ctl
Soil moisture (land only)	2.9%	2.5%	3.73	2.75	1.98	1.24	2.2%	1.9%	5.08	3.29	2.70	1.88
Precipitation (P)	3.8%	3.8%	5.04	5.29	2.70	3.41	4.0%	3.8%	6.03	4.18	3.41	1.88
Evaporation (E)	2.0%	1.7%	5.70	4.68	2.99	3.05	2.4%	2.1%	5.95	5.10	3.24	3.22
Sensible heat flux	3.8%	3.4%	5.05	4.76	3.00	2.61	4.7%	4.1%	4.60	2.91	2.26	1.49
E − P	8.5%	8.2%	6.15	5.59	3.35	3.78	10.6%	10.3%	6.45	3.68	3.40	1.84
200-mb height	6.0 m	8.6 m	1.04	6.75	0.38	2.37	6.2 m	6.7 m	6.74	6.03	2.39	1.46
500-mb height	5.5 m	5.8 m	4.15	5.53	2.97	1.53	5.6 m	5.5 m	8.54	5.30	1.69	1.89
850-mb height	4.2 m	3.1 m	8.14	4.15	6.04	1.52	3.7 m	3.2 m	6.07	1.00	1.14	0.44
200-mb temperature	0.25°C	0.24°C	3.15	4.66	0.00	0	0.23°C	0.14°C	8.15	1.36	3.49	0.53
500-mb temperature	0.16°C	0.22°C	0.89	5.79	0.02	2.23	0.18°C	0.17°C	7.49	5.69	1.99	2.42
850-mb temperature	0.23°C	0.36°C	2.61	5.83	0.14	1.11	0.27°C	0.26°C	*10.78*	***13.84***	3.18	4.81
2-m air temperature	0.26°C	0.34°C	3.68	7.77	1.49	4.64	0.28°C	0.24°C	9.28	4.96	5.78	2.43
SST (ocean only)	0.12°C	0.14°C	8.14	*10.94*	2.29	4.04	0.11°C	0.13°C	6.88	8.24	3.85	3.87
200-mb ucomp	0.51 m s^{-1}	0.49 m s^{-1}	1.79	2.25	0.70	1.35	0.54 m s^{-1}	0.51 m s^{-1}	8.46	5.86	2.63	3.49
500-mb ucomp	0.46 m s^{-1}	0.43 m s^{-1}	3.10	2.91	0.49	0.67	0.42 m s^{-1}	0.43 m s^{-1}	8.03	3.54	2.09	2.23
850-mb ucomp	0.30 m s^{-1}	0.32 m s^{-1}	4.17	5.83	1.43	2.99	0.23 m s^{-1}	0.26 m s^{-1}	6.41	8.21	2.36	2.48
10-m ucomp	0.14 m s^{-1}	0.14 m s^{-1}	3.76	6.14	1.69	3.36	0.12 m s^{-1}	0.11 m s^{-1}	4.64	1.84	2.37	0.82
200-mb vcomp	0.36 m s^{-1}	0.37 m s^{-1}	1.63	5.73	0.31	1.22	0.41 m s^{-1}	0.34 m s^{-1}	*9.91*	1.87	3.15	0.45
500-mb vcomp	0.31 m s^{-1}	0.32 m s^{-1}	3.21	5.54	1.13	1.07	0.34 m s^{-1}	0.27 m s^{-1}	8.26	1.25	1.81	0.52
850-mb vcomp	0.19 m s^{-1}	0.24 m s^{-1}	4.95	7.06	2.75	1.91	0.17 m s^{-1}	0.20 m s^{-1}	3.40	8.36	1.01	2.59
10-m vcomp	0.10 m s^{-1}	0.09 m s^{-1}	4.83	3.67	2.07	2.07	0.09 m s^{-1}	0.08 m s^{-1}	4.82	2.75	2.52	1.37
No. > 12.5%			0	0	0	0			0	1	0	0

TABLE 1. *(Continued)*

	JJA						SON					
	Mean absolute differences (% of Ctl for top 5 lines, physical units for others)		Passes standard test (% area)		Passes modified test (% area)		Mean absolute differences (% of Ctl for top 5 lines, physical units for others)		Passes standard test (% area)		Passes modified test (% area)	
Variable	Ctl2 − Ctl1	Def-Ctl	Ctl2 − Ctl1	Def − Ctl	Ctl2 − Ctl1	Def − Ctl	Ctl2 − Ctl1	Def − Ctl	Ctl2 − Ctl1	Def − Ctl	Ctl2 − Ctl1	Def − Ctl
Soil moisture (land only)	4.6%	3.6%	7.10	3.97	4.47	2.66	5.3%	3.9%	*11.88*	5.00	9.28	3.00
Precipitation (P)	5.4%	4.9%	7.94	5.85	5.12	3.07	4.2%	3.9%	6.71	3.62	3.86	1.87
Evaporation (E)	3.5%	3.6%	7.42	6.83	4.24	3.83	2.6%	2.3%	7.10	5.75	3.39	2.95
Sensible heat flux	4.7%	4.0%	9.38	7.49	5.98	4.57	4.7%	4.4%	7.00	6.27	4.19	3.84
E − P	10.3%	10.1%	8.03	7.55	5.05	4.44	8.5%	8.3%	4.80	3.54	2.35	2.00
200-mb height	7.5 m	5.3 m	***26.71***	7.02	***17.29***	3.29	7.2 m	6.6 m	***13.23***	4.77	3.30	2.42
500-mb height	4.4 m	4.4 m	***17.21***	***12.51***	*10.81*	7.60	5.2 m	5.2 m	*11.52*	6.83	1.79	1.94
850-mb height	2.7 m	3.3 m	*10.50*	***18.23***	4.31	***13.51***	2.9 m	3.4 m	4.25	5.45	0.13	1.87
200-mb temperature	0.18°C	0.17°C	***15.42***	***12.69***	7.01	7.22	0.13°C	0.14°C	2.52	3.64	0.60	2.10
500-mb temperature	0.19°C	0.14°C	***23.93***	8.00	*12.26*	4.17	0.18°C	0.17°C	***12.89***	6.04	4.45	3.50
850-mb temperature	0.22°C	0.22°C	***16.24***	***12.99***	9.10	2.38	0.24°C	0.27°C	***13.79***	***13.69***	3.26	4.17
2-m air temperature	0.21°C	0.16°C	***17.23***	7.60	*11.52*	4.74	0.28°C	0.23°C	***19.69***	9.33	***12.74***	5.05
SST (ocean only)	0.16°C	0.13°C	***21.84***	7.67	***14.86***	4.48	0.15°C	0.14°C	***22.83***	***14.71***	***14.29***	7.38
200-mb ucomp	0.66 m s^{-1}	0.60 m s^{-1}	***19.77***	*12.22*	*11.65*	7.43	0.57 m s^{-1}	0.53 m s^{-1}	7.25	5.96	0.79	2.54
500-mb ucomp	0.43 m s^{-1}	0.42 m s^{-1}	***17.77***	***13.39***	*12.08*	8.07	0.41 m s^{-1}	0.37 m s^{-1}	6.93	2.49	0.93	0.65
850-mb ucomp	0.24 m s^{-1}	0.25 m s^{-1}	***12.64***	***16.19***	6.77	6.17	0.22 m s^{-1}	0.24 m s^{-1}	5.27	7.88	1.11	2.40
10-m ucomp	0.11 m s^{-1}	0.10 m s^{-1}	7.87	9.44	4.87	5.76	0.12 m s^{-1}	0.10 m s^{-1}	3.75	2.36	1.74	1.52
200-mb vcomp	0.46 m s^{-1}	0.38 m s^{-1}	***13.90***	7.05	7.42	3.93	0.42 m s^{-1}	0.46 m s^{-1}	*10.91*	8.10	4.00	5.00
500-mb vcomp	0.33 m s^{-1}	0.30 m s^{-1}	*12.28*	7.77	6.49	4.47	0.35 m s^{-1}	0.36 m s^{-1}	*12.35*	8.29	3.33	4.94
850-mb vcomp	0.17 m s^{-1}	0.19 m s^{-1}	7.91	***12.52***	4.24	5.34	0.21 m s^{-1}	0.24 m s^{-1}	8.06	*12.43*	1.98	4.91
10-m vcomp	0.09 m s^{-1}	0.10 m s^{-1}	8.12	7.36	5.42	4.00	0.10 m s^{-1}	0.12 m s^{-1}	4.87	7.00	1.77	5.17
No. > 12.5%			11	7	2	1			5	2	2	0

TABLE 2. Same as in Table 1, but for the southern extratropics (south of 30°S).

	DJF						MAM					
	Mean absolute differences (% of Ctl for top 5 lines, physical units for others)		Passes standard test (% area)		Passes modified test (% area)		Mean absolute differences (% of Ctl for top 5 lines, physical units for others)		Passes standard test (% area)		Passes modified test (% area)	
Variable	Ctl2 − Ctl1	Def − Ctl	Ctl2 − Ctl1	Def − Ctl	Ctl2 − Ctl1	Def − Ctl	Ctl2 − Ctl1	Def − Ctl	Ctl2 − Ctl1	Def − Ctl	Ctl2 − Ctl1	Def − Ctl
Soil moisture (land only)	17.9%	5.0%	0.92	3.06	0.40	1.63	15.9%	4.9%	0.53	0.52	0.38	0.52
Precipitation (P)	3.6%	4.1%	3.38	6.05	1.83	3.38	3.3%	3.1%	7.48	6.08	5.20	3.46
Evaporation (E)	2.5%	3.0%	3.84	8.6	2.09	4.99	2.1%	1.9%	6.89	4.96	4.34	3.03
Sensible heat flux	5.2%	5.7%	4.90	8.31	2.49	4.41	4.9%	4.5%	4.89	5.38	2.76	2.95
E − P	6.5%	6.9%	3.15	4.73	1.36	2.19	7.3%	7.1%	6.96	6.72	4.03	3.91
200-mb height	7.3 m	5.6 m	3.58	8.41	0.90	2.04	9.3 m	8.0 m	***22.87***	***16.69***	2.47	*10.06*
500-mb height	5.1 m	4.4 m	1.19	5.85	0.00	0.94	7.7 m	5.8 m	***21.04***	***14.22***	2.52	8.16
850-mb height	3.9 m	3.2 m	0.83	7.51	0.00	1.4	5.3 m	3.4 m	***15.13***	*10.04*	1.53	4.83
200-mb temperature	0.11°C	0.22°C	2.28	***23.03***	1.09	***13.21***	0.12°C	0.10°C	7.29	7.09	2.76	5.53
500-mb temperature	0.14°C	0.15°C	3.75	*10.72*	0.56	4.34	0.16°C	0.17°C	9.06	***15.43***	3.98	8.25
850-mb temperature	0.11°C	0.14°C	6.42	7.38	1.26	3.87	0.13°C	0.20°C	3.71	***19.65***	0.68	6.22
2-m air temperature	0.10°C	0.12°C	7.79	*10.87*	3.13	6.24	0.18°C	0.17°C	8.22	*11.18*	4.74	5.52
SST (ocean only)	0.09°C	0.10°C	5.46	*11.54*	1.76	6.1	0.08°C	0.10°C	6.21	*10.08*	3.19	3.66
200-mb ucomp	0.56 m s^{-1}	0.54 m s^{-1}	3.71	4.83	1.25	1.41	0.66 m s^{-1}	0.52 m s^{-1}	***19.98***	*9.70*	4.57	4.84
500-mb ucomp	0.42 m s^{-1}	0.43 m s^{-1}	3.40	5.69	1.65	1.72	0.56 m s^{-1}	0.39 m s^{-1}	***20.18***	7.33	6.09	3.56
850-mb ucomp	0.29 m s^{-1}	0.33 m s^{-1}	2.37	5.36	1.31	1.4	0.45 m s^{-1}	0.34 m s^{-1}	***17.90***	*11.52*	6.26	2.77
10-m ucomp	0.17 m s^{-1}	0.17 m s^{-1}	2.18	6.01	0.69	2.67	0.28 m s^{-1}	0.16 m s^{-1}	***18.06***	3.80	*11.95*	1.61
200-mb vcomp	0.31 m s^{-1}	0.30 m s^{-1}	3.01	6.61	0.31	3.22	0.31 m s^{-1}	0.40 m s^{-1}	2.42	*12.03*	0.94	7.65
500-mb vcomp	0.22 m s^{-1}	0.23 m s^{-1}	4.41	9.04	0.72	4.58	0.28 m s^{-1}	0.31 m s^{-1}	5.42	***13.04***	2.27	9.45
850-mb vcomp	0.16 m s^{-1}	0.22 m s^{-1}	5.28	*12.12*	1.46	5.81	0.20 m s^{-1}	0.26 m s^{-1}	7.29	***15.52***	2.75	5.55
10-m vcomp	0.11 m s^{-1}	0.10 m s^{-1}	3.44	7.75	1.65	5.09	0.12 m s^{-1}	0.12 m s^{-1}	7.19	6.54	4.24	2.75
No. > 12.5%			0	1	0	1			7	6	0	0

TABLE 2. *(Continued)*

	JJA						SON					
	Mean absolute differences (% of Ctl for top 5 lines, physical units for others)		Passes standard test (% area)		Passes modified test (% area)		Mean absolute differences (% of Ctl for top 5 lines, physical units for others)		Passes standard test (% area)		Passes modified test (% area)	
Variable	Ctl2 − Ctl1	Def − Ctl	Ctl2 − Ctl1	Def − Ctl	Ctl2-Ctl1	Def − Ctl	Ctl2 − Ctl1	Def − Ctl	Ctl2 − Ctl1	Def − Ctl	Ctl2 − Ctl1	Def − Ctl
Soil moisture (land only)	11.5%	3.7%	0.80	0.92	0.40	0.24	11.0%	3.5%	0.69	0.00	0.47	0.00
Precipitation (P)	3.0%	2.7%	5.55	3.65	3.27	2.16	2.9%	3.6%	3.54	8.00	1.39	5.16
Evaporation (E)	1.9%	1.8%	4.43	4.64	2.31	2.31	2.1%	1.9%	3.47	2.09	1.45	0.97
Sensible heat flux	4.1%	3.4%	5.35	3.90	3.72	2.33	4.4%	4.6%	2.58	3.58	1.09	1.72
E − P	6.9%	6.3%	5.31	4.14	2.94	2.02	6.3%	7.8%	2.89	6.16	0.88	4.00
200-mb height	6.2 m	5.2 m	2.28	1.55	0.82	0.90	4.3 m	8.0 m	0.00	*11.31*	0.00	7.83
500-mb height	5.0 m	4.3 m	1.45	0.78	0.13	0.17	3.4 m	5.7 m	0.00	*12.10*	0.00	8.96
850-mb height	3.5 m	3.1 m	3.74	2.54	1.36	0.91	2.3 m	4.6 m	0.00	***15.77***	0.00	*11.94*
200-mb temperature	0.12°C	0.17°C	1.10	***14.69***	0.10	9.05	0.12°C	0.26°C	1.46	***13.03***	0.00	6.52
500-mb temperature	0.13°C	0.13°C	2.18	3.52	0.26	2.17	0.10°C	0.13°C	0.98	7.67	0.11	5.76
850-mb temperature	0.15°C	0.17°C	3.24	*11.28*	1.87	2.68	0.12°C	0.19°C	4.04	***15.36***	1.66	4.54
2-m air temperature	0.19°C	0.17°C	6.46	6.56	3.72	3.16	0.13°C	0.13°C	3.54	9.21	0.93	3.63
SST (ocean only)	0.08°C	0.09°C	7.15	9.46	4.53	4.42	0.07°C	0.09°C	6.55	*9.86*	2.58	4.11
200-mb ucomp	0.47 m s^{-1}	0.48 m s^{-1}	5.16	4.04	3.18	1.78	0.38 m s^{-1}	0.62 m s^{-1}	0.71	*11.70*	0.00	*10.02*
500-mb ucomp	0.37 m s^{-1}	0.36 m s^{-1}	5.00	1.89	2.60	0.40	0.30 m s^{-1}	0.48 m s^{-1}	0.03	*11.50*	0.00	*9.70*
850-mb ucomp	0.26 m s^{-1}	0.36 m s^{-1}	4.64	*11.10*	2.38	3.17	0.21 m s^{-1}	0.47 m s^{-1}	0.00	***20.67***	0.00	*12.24*
10-m ucomp	0.16 m s^{-1}	0.19 m s^{-1}	5.92	5.05	4.07	3.07	0.13 m s^{-1}	0.23 m s^{-1}	0.42	***14.56***	0.09	*11.81*
200-mb vcomp	0.35 m s^{-1}	0.31 m s^{-1}	2.80	4.70	1.01	2.43	0.23 m s^{-1}	0.39 m s^{-1}	0.00	*10.54*	0.00	5.75
500-mb vcomp	0.28 m s^{-1}	0.25 m s^{-1}	2.09	6.15	0.38	3.32	0.17 m s^{-1}	0.28 m s^{-1}	0.04	*10.05*	0.00	5.11
850-mb vcomp	0.21 m s^{-1}	0.24 m s^{-1}	3.40	*10.48*	0.94	3.08	0.12 m s^{-1}	0.31 m s^{-1}	0.00	***17.17***	0.00	6.84
10-m vcomp	0.12 m s^{-1}	0.11 m s^{-1}	5.19	4.23	2.50	2.17	0.08 m s^{-1}	0.13 m s^{-1}	1.59	6.89	0.32	3.52
No. > 12.5%			0	1	0	0			0	6	0	0

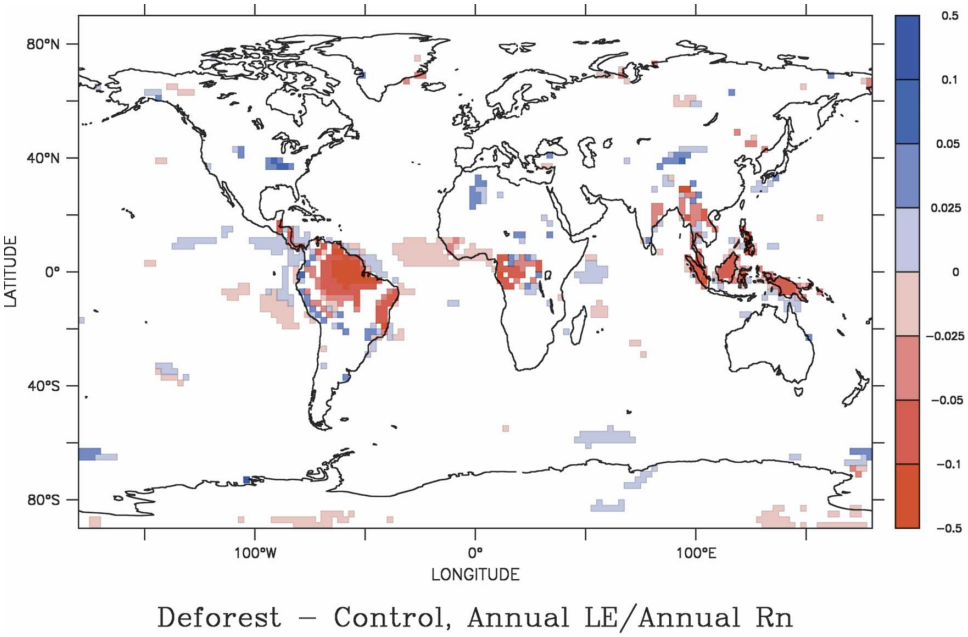

FIG. 4. Differences in annual mean latent heat (LE) divided by annual mean net radiation (Rn) between the deforestation and control runs. Differences are only shown where differences in LE are significant according to the modified t test at the 95% level. Red shading indicates areas with less evapotranspiration in the deforested run than in the control run.

warming in most of the Amazon and small portions of central Africa and Oceania (Fig. 5). Evaporation decreases by about 0.1 cm day^{-1} in the annual mean in the deforested regions, and annual mean sensible heat flux increases by up to 25 W m^{-2} in the Amazon, and by up to 10 W m^{-2} in central Africa and Oceania.

The precipitation responses (and therefore the atmospheric latent heating responses) to the deforestation

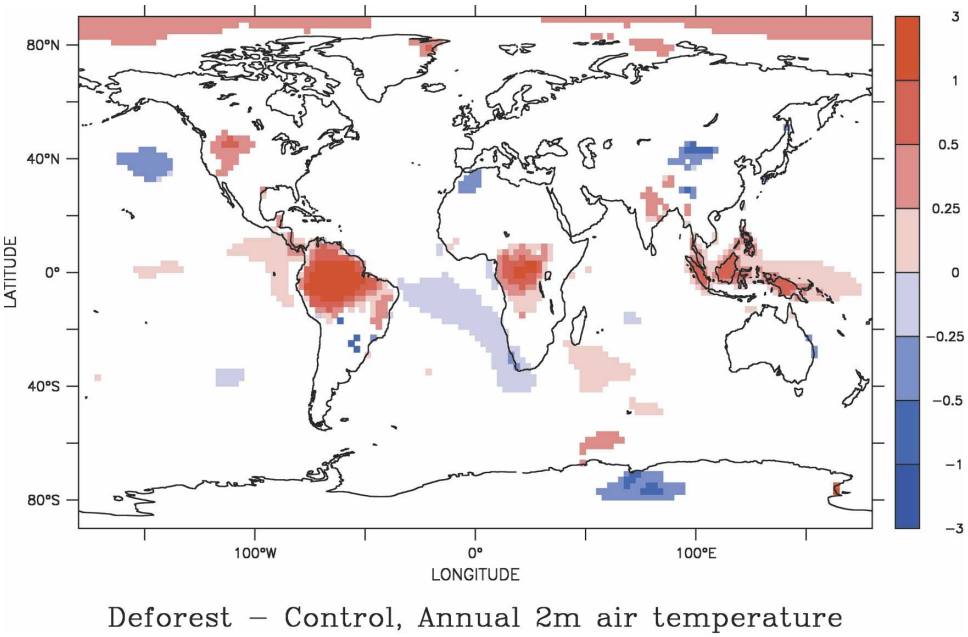

FIG. 5. Same as in Fig. 4, but for 2-m reference temperature (°C), with red shading indicating warming in the deforested scenario.

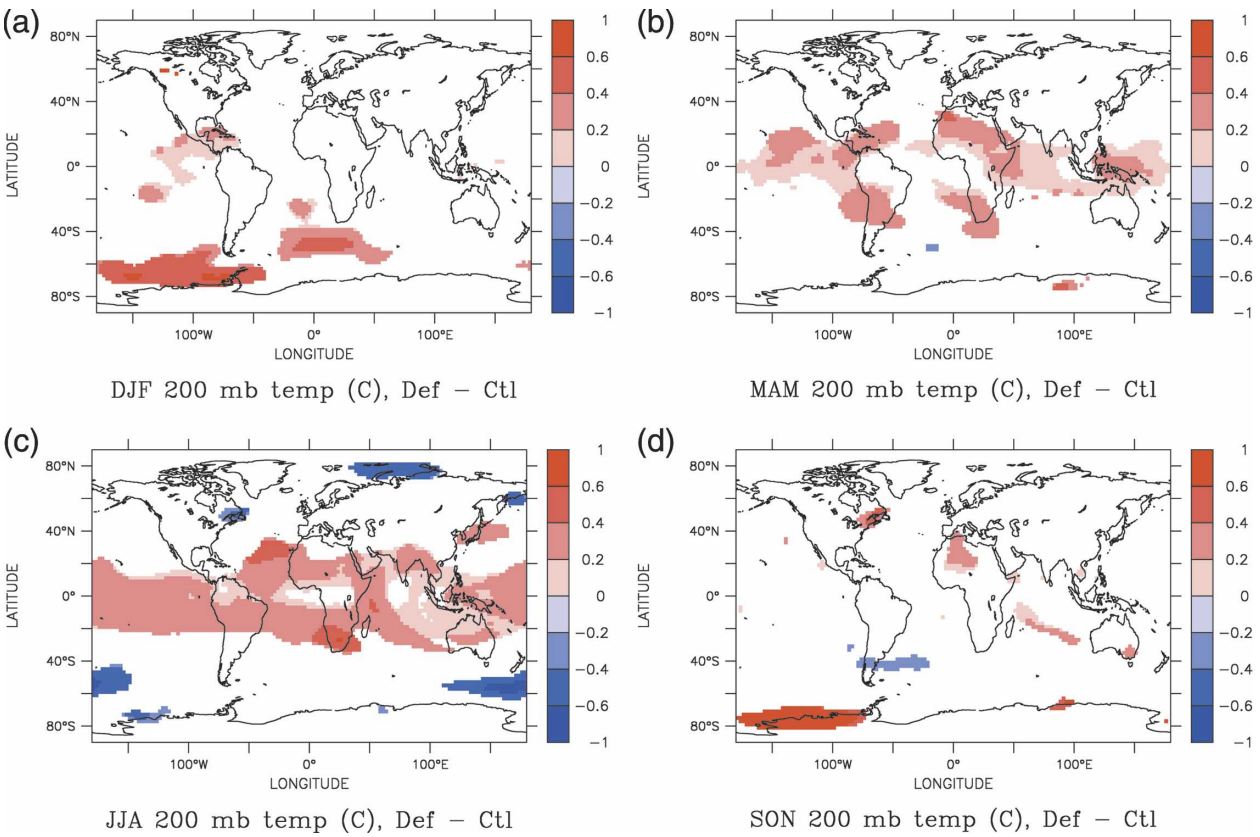

FIG. 6. Differences in 200-mb temperature (°C) between the deforestation and control runs (DEF – CTL) for seasons (a) DJF, (b) MAM, (c) JJA, and (d) SON. Only those differences significant at the 95% level are shown. Red shading indicates warming in the deforested run.

scenario vary from region to region and from season to season (Fig. 8). As stated earlier, a detailed account of the behavior of each region will be provided in a separate publication: the focus of this manuscript is on the extratropical response. It is worth noting, however, that the localized temperature, ET, and precipitation changes seen in the current experiment are comparable to changes documented in earlier tropical deforestation studies. McGuffie et al. (1995) list changes for the Amazon region for nine studies from the late 1980s to the mid-1990s (their Table 1). The mean (median) differences from those studies show a deforested Amazon basin that is 1.55°C (2.0°C) warmer, has 290 mm yr^{-1} (335 mm yr^{-1}) less precipitation, and 333 mm yr^{-1} (231 mm yr^{-1}) less ET. The range of results for these nine studies was quite large, with temperature differences ranging from −0.11° to 3.8°C (only one model showed a temperature decrease), and precipitation differences ranging from a reduction of 640 mm yr^{-1} to an increase of 394 mm yr^{-1} (only one model showed a precipitation increase). All the models showed decreased evapotranspiration, with differences ranging from 985 to 164 mm yr^{-1}. Later studies by Zhang et al. (1996a) and Lean and Rowntree (1999) found differences within the range of the earlier studies: 0.3°C warmer, 402 mm yr^{-1} less precipitation, and 222 mm yr^{-1} less ET for the former study, and 1.73°C warmer, 139 mm yr^{-1} less precipitation, and 259 mm yr^{-1} less ET for the latter. The results from our experiment are also within the range of these earlier studies: 1.0°C warmer, 159 mm yr^{-1} less precipitation, and 175 mm yr^{-1} less ET.

The localized surface warming in each of the deforested regions (Fig. 5) is accompanied by a broad, mild warming throughout the tropical troposphere, with temperature increases typically between 0.1° and 0.2°C at levels from 700 to 150 mb (Fig. 6: 200-mb temperature differences for all four seasons). The broad, mild warming in the Tropics is significant in March–May (MAM) and JJA. This warming is accompanied by a broad increase in 200-mb geopotential heights, also significant in MAM and JJA (Fig. 7). Tropospheric vertical velocity increases in all seasons except SON in the deforested regions, with the largest increases in December–February (DJF), and shows smaller magnitude de-

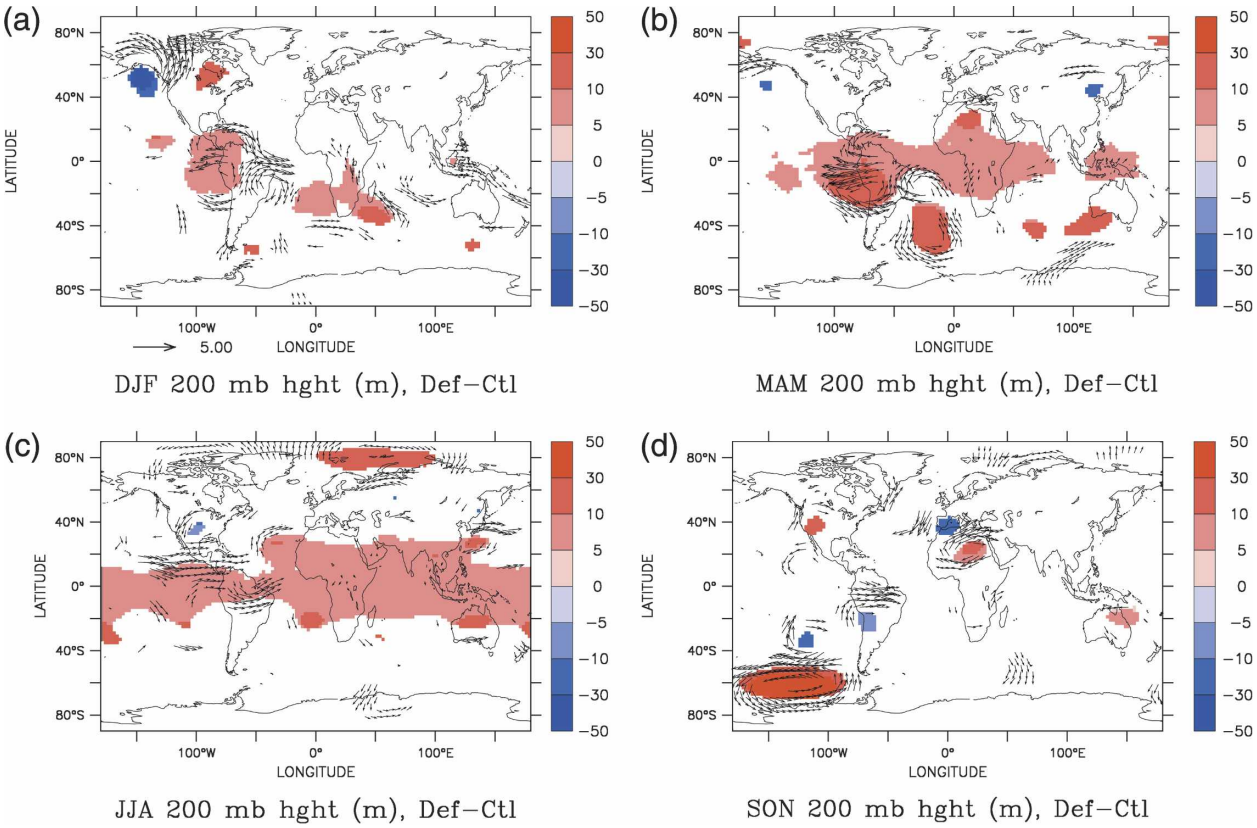

FIG. 7. Same as in Fig. 6, but for 200-mb geopotential height differences (m), with 200-mb wind vector anomalies superimposed. Wind scale vector of 5 m s^{-1} appears below upper-left plot. Red shading indicates geopotential height increases in the deforested run.

creases north and east of the deforested regions. Significant changes in vertical velocity do not extend beyond the Tropics. Other fields associated with the Walker and Hadley circulations do not show changes in the deforestation–control comparison that differ appreciably from those in the control–control comparison. This is in contrast to the results of Zhang et al. (1996b), who discussed the possibility that changes in the Walker and Hadley circulations caused by tropical deforestation could produce global-scale impacts.

The percentage area of the northern and southern extratropics (north of 30°N and south of 30°S), respectively, that passes the standard and the modified *t* tests at the 95% level for 21 different variables for each of the four seasons are listed in Tables 1 and 2. The tables show that the percent area passing either *t* test in the comparison between the deforestation and the control experiment is within the range of values seen among all the different comparisons between two segments of the control experiment. For the hydroclimatic variables listed in the top five lines of the tables, only 1 of 40 values listed has an area of significance greater than 5% for the modified test for the deforestation–control comparison (5.16% for SON precipitation in the southern extratropics). In contrast, 5 of these 40 values exceed 5% for the control–control comparison, but only 1 is greater than 6% (9.28% for northern extratropical SON soil moisture). The mean absolute differences (e.g., the mean absolute value of precipitation in the deforested run minus precipitation in the control run, divided by the mean control run value, expressed in a percentage) are generally between 2% and 6% of the control run mean value in both of the comparisons. (The Southern Hemisphere soil moisture has higher normalized difference percentages, particularly in the control–control comparison, but this is a result of small sample size due to the small extent of nonglaciated land area south of 30°S; very little area passes either significance test.)

Given the Livezey and Chen (1983)–based requirements for field significance discussed in section 4b, it is unlikely that any of the hydroclimatic fields would pass a stringent field significance test. As stated above, fields with even 1000 dof require about 6% of the field to pass independent 95% level significance tests for the field as a whole to be considered significant at the 95% level.

The literature reported in the appendix indicates that there are far fewer than 1000 dof for all of the variables listed in the tables. The reported dof values range from about 20 to about 100, depending on the variable, season, and spatial and temporal scales. The number of variables exceeding 12.5% is tallied below each column in Tables 1 and 2 under the assumption that 40 dof is the most representative value, based on the literature cited in the appendix. No value on the top five lines exceeds even the 9.5% criterion associated with 100 dof.

Both comparisons show larger areas of geopotential height and temperature fields (second group of eight variables in Tables 1 and 2) and wind fields (third group of eight variables in Tables 1 and 2) passing the significance tests than the areas related to the hydrologic variables. This is consistent with the general tendency for these second and third groups of variables to have larger spatial correlation scales (and fewer dof) than the tabulated hydrologic variables. The number of these variables with more than 5% or 9.5% of the area passing the modified significance test is similar between the two comparisons in three seasons in the northern extratropics (DJF, MAM, SON) and one season in the southern extratropics (JJA). The JJA results for the deforestation–control comparison in the northern extratropics has 8 of these 16 temperature and wind fields showing at least 5% of the area passing (1 of these exceeds the 12.5% threshold associated with 40 dof), while 13 of these same 16 fields exceed the 5% areal significance in the control–control comparison (7 of these exceed the 9.5% threshold and 2 exceed the 12.5% threshold). In the southern extratropics, however, all seasons except JJA have many more variables with greater than 5% passing the modified test in the deforestation–control comparison than in the control–control comparison, but only in SON does this difference hold when the 9.5% threshold is considered for field significance (5 versus 0 fields passing). In all the seasons, only the 200-mb temperature in the deforestation–control comparison has enough area to pass the 12.5% threshold associated with 40 dof (13.2% passes). No field passes this threshold in the control–control comparison.

When the results of the standard t test are considered, northern JJA and SON and southern MAM and SON have more than 1 field passing the 12.5% threshold for field significance for fields with 40 dof (bottom row in Tables 1 and 2). In three of these seasons, there are more exceedances in the control–control comparison than in the deforestation–control comparison (11 versus 7, 5 versus 2, and 7 versus 6, respectively; Southern SON has 0 versus 6), suggesting that the extratropical variation observed between the deforestation and the control experiments is within the range of variation observed within the control experiment.

In summary, the model results presented here show that though local tropical responses to deforestation may be extensive, extratropical responses are generally small in magnitude and, with a few noted exceptions, not statistically significant. Essentially no statistically significant responses were simulated in the Northern Hemisphere extratropics. In the Southern Hemisphere extratropics, no statistically significant changes were simulated in any hydrologic fields. A few localized areas with possibly statistically significant temperature and wind anomalies were simulated in the Southern Hemisphere extratropics during some seasons when all tropical broadleaf evergreen forests of the Amazon, central Africa, and the islands of Oceania were completely deforested. However, a similar comparison of two 50-yr segments of the control run yields differences of the same magnitudes and the same apparent significance.

An earlier version of the same model, only slightly different from the one discussed here, was used in four separate deforestation experiments: one with the same deforestation scenario reported here, and three more with each of the tropical broadleaf evergreen forest zones individually deforested while the others were left intact. In all cases, the 50-yr comparison periods began after equilibration periods of at least 10 yr. The results of the complete conversion were similar to the results presented here, and even less of a significant extratropical signal was detected in each of the simulations with only one tropical region deforested.

6. Discussion

Shukla et al. (1990), Henderson-Sellers et al. (1993), and Zhang et al. (1996b) emphasize the global implications of extensive tropical deforestation. They suggest that changes in the Walker and Hadley circulations could lead to significant extratropical responses, and the latter two studies report such changes. As mentioned in the introduction, computer resources greatly limited the extent of each of the simulations in these earlier studies. Zhang et al. (1996b) recognized this with the statement "it might be that the model simulated changes in mid- and high latitudes are the result of poor representation of the physical processes in the model or its natural variability rather than being induced by the tropical deforestation" (p. 2514). Through the long-term averaging and the statistical testing presented above, we believe that we have demonstrated that in our model, the extratropics are not highly sen-

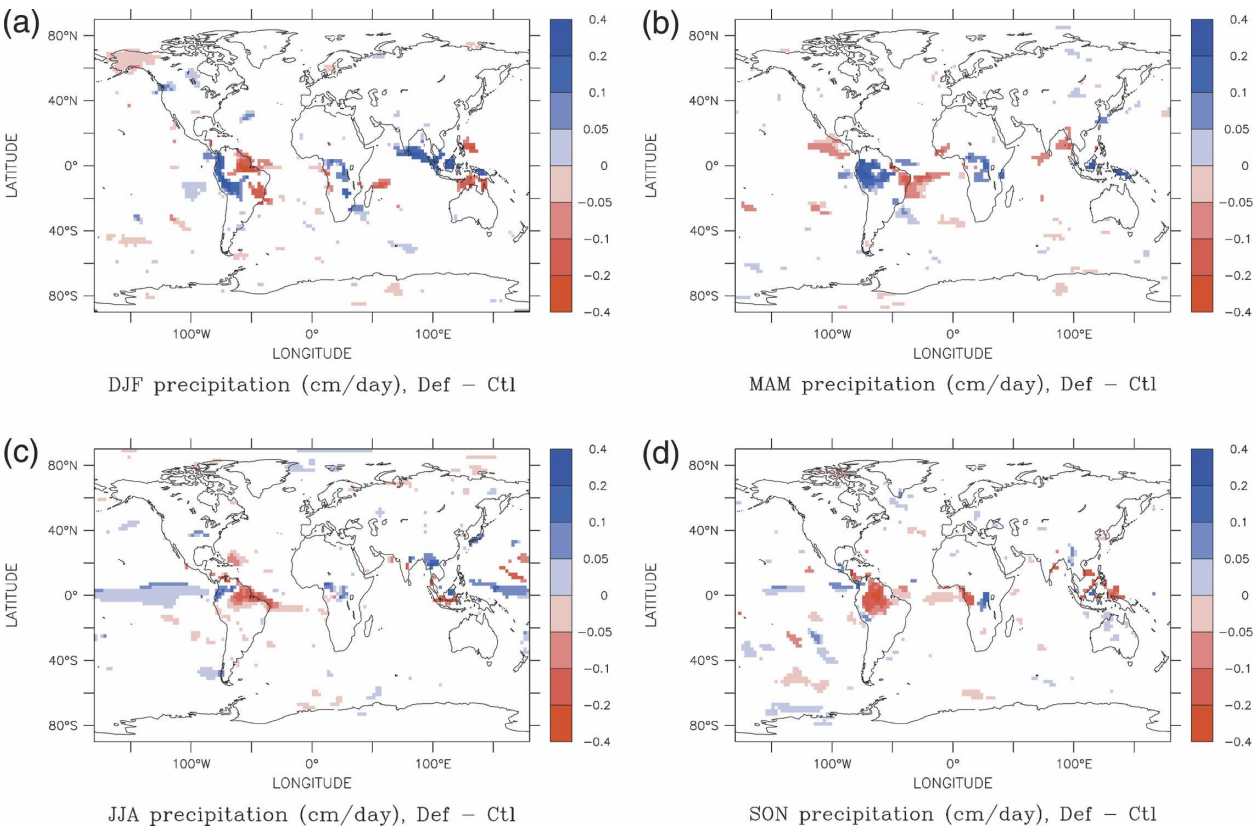

FIG. 8. Same as in Fig. 6, but for precipitation differences (cm day^{-1}). Red shading indicates less precipitation in the deforested run.

sitive to tropical deforestation. The northern extratropics in particular show no significant response to the imposed deforestation, and the southern extratropics show only a few small but possibly significant regional changes, especially in the southeastern Pacific.

The findings presented here are further supported by additional experiments (not shown, performed with an earlier version of the model used in this study) showing that deforestation of one continent at a time yields even smaller extratropical changes than deforesting all three continents at once, and yields no statistically significant extratropical signal in any field.

One rationale for studies of tropical deforestation has been the similarity between the potential surface heating anomalies induced by tropical deforestation and the high sea surface temperatures of an El Niño event. Eltahir and Bras (1993) discuss why these two situations are not inherently equivalent. In an El Niño event, the surface heating increase is generally spatially coincident with a precipitation increase, both of which contribute anomalous heating to the atmosphere. Thus, the two processes act in concert to exert a large signal that can significantly impact tropical circulation. In contrast, surface temperature and precipitation changes do not always act in this manner in response to tropical deforestation: in many GCM representations of the problem, precipitation is reduced after deforestation, yielding a surface heat source and the equivalent of an upper-level heat sink. The lack of a spatially coherent tropical precipitation signal probably leads to the relatively minor extratropical response noted here. Though the surface temperature response is always positive in this model (hotter after deforestation, Fig. 5), the precipitation response is seasonally and spatially dependent (Fig. 8).

One limitation of the current study is the use of a slab ocean model, which lacks ocean dynamics. Because a fully coupled model with ocean dynamics would respond to wind stress changes more realistically than a slab ocean model, one could anticipate a different outcome from a fully coupled model, particularly if the surface wind stress changes were large (e.g., Delire et al. 2001). In these experiments, surface wind anomalies are significant in less than one-quarter of the Tropics (for the zonal component of the 10-m reference winds, 19%–25% of the Tropics passes the modified significance test at the 95% level in each season). Where the surface wind differences are significant, they are small

in magnitude (generally less than 0.5 m s^{-1} over the tropical oceans, up to 1 m s^{-1} different over the deforested regions in Africa and Oceania, up to 2 m s^{-1} over Amazonia). The small magnitude of the tropical surface wind anomalies observed in these experiments suggests that a fully coupled model would not produce substantially different results.

An additional factor that was not included in the simulations discussed above is the release of carbon that would accompany such large-scale deforestation. This would affect the climate through radiative forcing effects (CO_2, biomass burning aerosols, etc.) as well as interactive carbon-cycle effects on vegetation physiology (i.e., changes in stomatal conductance). Claussen et al. (2001), Matthews et al. (2004), and Brovkin et al. (2004) find that the inclusion of carbon emissions in various land-cover change experiments increases global temperatures.

7. Conclusions

The AM2/LM2 version of the GFDL GCM coupled to a slab ocean model has been used to investigate extratropical responses to tropical deforestation. Lengthy integrations and statistical tools that account for temporal correlation and field significance have been used to show that though local tropical responses to deforestation may be extensive, extratropical responses are generally small in magnitude, and, with a few noted exceptions, not statistically significant. Conversion of all tropical broadleaf evergreen forests of the Amazon, central Africa, and the islands of Oceania to grassland yielded essentially no statistically significant responses in the Northern Hemisphere extratropics. In the Southern Hemisphere extratropics, no statistically significant changes were simulated in any hydrologic fields. A few localized areas with possibly statistically significant temperature and wind anomalies were simulated in the Southern Hemisphere extratropics during some seasons. However, a similar comparison of two 50-yr segments of the control run yields differences of the same magnitudes and the same apparent significance. This leads us to conclude that according to the GFDL model, extratropical responses to complete tropical deforestation (ignoring greenhouse gas effects) are unlikely to be distinguishable from natural climate variability on a time scale of 50 yr.

Acknowledgments. The authors thank Rich Gudgel for running the control simulation and sharing the results of this run, and Lori Thompson for her assistance debugging some of the programs used in this work. Insightful reviews and helpful suggestions were provided by John Lanzante, Elena Shevliakova, Greg McCabe, and three anonymous reviewers.

APPENDIX

Estimates of Spatial Degrees of Freedom

Livezey and Chen (1983) report about 55 and 35 dof for summer and winter, respectively, 700-mb height anomalies from 20° to 80°N from a 30-yr dataset. From a separate study of a 40-yr record of winter mean and annual mean temperature and precipitation for the United States, they estimate that the temperature dataset contains on the order of 10 dof, and the precipitation dataset contains less than 50 dof. Bretherton et al. (1999) report 20 to 25 dof for Northern Hemisphere winter (DJF) 500-mb height. Fraedrich et al. (1995) report about 25–35 dof for monthly means of 1000-mb height for the region between 30.5° and 74.7°N. The larger values are reported in the summer months, and the smaller values in the winter months. Wang and Shen (1999) use four different methods to estimate spatial dof. They determine that the binomial method of Livezey and Chen (1983) provides the best estimates. For Northern Hemisphere monthly surface temperature, Wang and Shen (1999) find a seasonal cycle of dof ranging from about 60 in the winter months to about 90 in the summer months. In the Southern Hemisphere, they find a different seasonal cycle with dof ranging from about 50 in the winter months to about 35 in the summer months. Van den Dool and Chervin (1986) provide estimates of dof for about 10 variables on annual time scales for the entire globe, the Northern and Southern Hemispheres, and north of 20°N. For the region north of 20°N, they also provide estimates of dof for three variables on monthly scales. For this region, the annual results include estimates from 18 to 21 dof for geopotential height at four different levels, 34 dof for 700-mb temperature, 30 dof for 300-mb zonal wind, 110 dof for meridional flux of 300-mb zonal momentum by transient eddies, and 78 dof for meridional flux of 850-mb temperature by transient eddies. The monthly data for this region range from about 10 to 42 dof for both surface pressure and 500-mb geopotential height, with smaller values in the fall and winter, and higher values in the spring and summer. For the thickness of the layer between 500 and 1000 mb, the dof range from 16 to 55, again with higher values in the summer months. Van den Dool (1987) reports about 57 dof for the combined precipitation and vertical motion anomaly field over the continental United States.

REFERENCES

Bretherton, C. S., M. Widmann, V. P. Dymnikov, J. M. Wallace, and I. Bladé, 1999: The effective number of spatial degrees of freedom of a time-varying field. *J. Climate,* **12,** 1990–2009.

Broccoli, A. J., 2000: Tropical cooling at the Last Glacial Maximum: An atmosphere-mixed layer ocean model simulation. *J. Climate,* **13,** 951–976.

Brovkin, V., S. Sitch, W. Von Bloh, M. Claussen, E. Bauer, and W. Cramer, 2004: Role of land cover changes for atmospheric CO_2 increase and climate change during the last 150 years. *Global Change Biol.,* **10,** 1253–1266.

Chase, T. N., R. A. Pielke Sr., T. G. F. Kittel, R. R. Nemani, and S. W. Running, 2000: Simulated impacts of historical land cover changes on global climate in Northern winter. *Climate Dyn.,* **16,** 93–105.

Claussen, M., V. Brovkin, and A. Ganopolski, 2001: Biogeophysical versus biogeochemical feedbacks of large-scale land cover change. *Geophys. Res. Lett.,* **28,** 1011–1014.

Delire, C., P. Behling, M. T. Coe, J. A. Foley, R. Jacob, J. Kutzbach, Z. Liu, and S. Vavrus, 2001: Simulated response of the atmosphere-ocean system to deforestation in the Indonesian Archipelago. *Geophys. Res. Lett.,* **28,** 2081–2084.

Delworth, T. L., and Coauthors, 2006: GFDL's CM2 global coupled climate models. Part I: Formulation and simulation characteristics. *J. Climate*, **19,** 643–674.

Dickinson, R. E., and A. Henderson-Sellers, 1988: Modelling tropical deforestation: A study of GCM land-surface parameterizations. *Quart. J. Roy. Meteor. Soc.,* **114,** 439–462.

Eltahir, E. A. B., and R. L. Bras, 1993: On the response of the tropical atmosphere to large-scale deforestation. *Quart. J. Roy. Meteor. Soc.,* **119,** 779–793.

Fraedrich, K., C. Ziehmann, and F. Sielmann, 1995: Estimates of spatial degrees of freedom. *J. Climate,* **8,** 361–369.

GFDL Global Atmospheric Model Development Team, 2004: The new GFDL Global Atmosphere and Land Model AM2–LM2: Evaluation with prescribed SST simulations. *J. Climate,* **17,** 4641–4673.

Hansen, J., A. Lacis, D. Rind, G. Russell, P. Stone, I. Fung, R. Ruedy, and J. Lerner, 1984: Climate sensitivity: Analysis of feedback mechanisms. *Climate Processes and Climate Sensitivity, Geophys. Monogr.,* Vol. 29, Amer. Geophys. Union, 130–163.

Henderson-Sellers, A., and V. Gornitz, 1984: Possible climatic impacts of land cover transformations, with particular emphasis on tropical deforestation. *Climate Change,* **6,** 231–257.

——, R. E. Dickinson, T. B. Durbridge, P. J. Kennedy, K. McGuffie, and A. J. Pitman, 1993: Tropical deforestation: Modeling local- to regional-scale climate change. *J. Geophys. Res.,* **98** (D4), 7289–7315.

Hurtt, G.C., S. Frolking, M.G. Fearon, B. Moore III, E. Shevliakova, S. Malyshev, S.W. Pacala, and R.A. Houghton, 2006: The underpinnings of land-use history: Three centuries of global gridded land-use transitions, wood harvest activity, and resulting secondary lands. *Global Change Biol*., in press.

Lean, J., and D. A. Warrilow, 1989: Simulation of the regional climatic impact of Amazon deforestation. *Nature,* **342,** 411–413.

——, and P. R. Rowntree, 1999: Correction note on "Understanding the sensitivity of a GCM simulation of Amazonian deforestation to the specification of vegetation and soil characteristics." *J. Climate,* **12,** 1549–1551.

Livezey, R. E., and W. Y. Chen, 1983: Statistical field significance and its determination by Monte Carlo techniques. *Mon. Wea. Rev.,* **111,** 46–59.

Matthews, H. D., A. J. Weaver, K. J. Meissner, N. P. Gillett, and M. Eby, 2004: Natural and anthropogenic climate change: Incorporating historical land cover change, vegetation dynamics and the global carbon cycle. *Climate Dyn.,* **22,** 461–479.

McGuffie, K., A. Henderson-Sellers, H. Zhang, T. B. Durbridge, and A. J. Pitman, 1995: Global climate sensitivity to tropical deforestation. *Global Planet. Change,* **10,** 97–128.

Milly, P. C. D., and A. B. Shmakin, 2002a: Global modeling of land water and energy balances. Part I: The land dynamics (LaD) model. *J. Hydrometeor.,* **3,** 283–299.

——, and ——, 2002b: Global modeling of land water and energy balances. Part II: Land-characteristic contributions to spatial variability. *J. Hydrometeor.,* **3,** 301–310.

Polcher, J., and K. Laval, 1994: The impact of African and Amazonia deforestation on tropical climate. *J. Hydrol.,* **155,** 389–405.

Shukla, J., C. Nobre, and P. Sellers, 1990: Amazon deforestation and climate change. *Science,* **247,** 1322–1325.

Sud, Y. C., G. K. Walker, J.-H. Kim, G. E. Liston, P. J. Sellers, and W. K.-M. Lau, 1996: Biogeophysical consequences of a tropical deforestation scenario: A GCM simulation study. *J. Climate,* **9,** 3225–3247.

Van den Dool, H. M., 1987: An empirical study on the parameterization of precipitation in a model of the time mean atmosphere. *J. Atmos. Sci.,* **44,** 224–235.

——, and R. M. Chervin, 1986: A comparison of month-to-month persistence of anomalies in a general circulation model and in the earth's atmosphere. *J. Atmos. Sci.,* **43,** 1454–1466.

Von Storch, H., and F. W. Zwiers, 1999: *Statistical Analysis in Climate Research.* Cambridge University Press, 484 pp.

Wang, X., and S. S. Shen, 1999: Estimation of spatial degrees of freedom of a climate field. *J. Climate,* **12,** 1280–1291.

Wilson, C. A., and J. F. B. Mitchell, 1987: A doubled CO_2 climate sensitivity experiment with a global climate model including a simple ocean. *J. Geophys. Res.,* **92** (D11), 13 315–13 343.

Winton, M., 2000: A reformulated three-layer sea ice model. *J. Atmos. Oceanic Technol.,* **17,** 525–531.

Zhang, H., K. McGuffie, and A. Henderson-Sellers, 1996a: Impacts of tropical deforestation. Part I: Process analysis of local climatic change. *J. Climate,* **9,** 1497–1517.

——, ——, and ——, 1996b: Impacts of tropical deforestation. Part II: The role of large-scale dynamics. *J. Climate,* **9,** 2498–2521.

Zwiers, W. F., and H. Von Storch, 1995: Taking serial correlation into account in tests of the mean. *J. Climate,* **8,** 336–351.